Structural transformations from point to extended defects in silicon: A molecular dynamics study

Luis A. Marqués,* Lourdes Pelaz, Iván Santos, Pedro López, and María Aboy
Departamento de Electrónica, E.T.S.I. de Telecomunicación, Universidad de Valladolid, 47011 Valladolid, Spain
(Received 21 July 2008; revised manuscript received 8 October 2008; published 11 November 2008)

We use classical molecular dynamics simulation techniques to study how point defects aggregate to form extended defects in silicon. We have found that ⟨110⟩ chains of alternating interstitials and bond defects, a generalization of the Si di-interstitial structure, are metastable at room temperature but spontaneously transform into {311} defects when annealed at higher temperatures. Obtained atomic configurations and energetics are in good agreement with experiments and previous theoretical calculations. We have found a {311} structural unit which consists of two interstitial chains along ⟨110⟩ but arranged differently with respect to the known {311} units.

DOI: 10.1103/PhysRevB.78.193201 PACS number(s): 61.72.Cc, 61.72.Nn, 61.82.Fk

Defect engineering in semiconductors is a topic of great interest. Ion implantation and annealing are key processing steps used for the fabrication of *p*-*n* junctions within the manufacturing industry of Si and Ge electronic devices. Besides the introduced dopant atoms, excess self-interstitials above equilibrium conditions are generated in the lattice. They form aggregates that tend to evolve through an Ostwald ripening process: larger defect clusters grow at the expense of interstitials freed from smaller and less stable agglomerates.[1] At sizes of several hundred interstitials these aggregates become visible in transmission electron microscopy (TEM) images, they show regular atomic structures, and are generally known as *extended defects*.[2] They act as a reservoir of interstitials that are slowly released during subsequent thermal treatments causing the transient enhanced diffusion of interstitial-diffusing dopants.[3] On the other hand, extended defects show photoluminiscent signals[4] and have been proposed to fabricate optical emitters compatible with the standard and well-established integrated-circuit technology. Extended defects introduce local strain fields, which modify the band structure and provide spatial confinement of the charge carriers allowing room-temperature electroluminescence.[5] For these reasons, the study of the formation and control of extended defects in semiconductors is of great importance, both from the fundamental and technological points of view.

Among interstitial-rich extended defects, {311} defects have received much attention because they are formed during implantation and annealing conditions relevant to Si processing.[3] The atomic structure of {311} defects was determined by Takeda[6] using TEM. They consist of large interstitial chains along the ⟨110⟩ direction, packed together along the {311} plane, which gives this defect its name. Its atomic model can be described as a sequence of structural units of three types: *I units*, which are two tiny rods of hexagonal Si containing the interstitial ⟨110⟩ chains; *O units*, eight-membered rings with no excess or deficit of atoms with respect to perfect lattice; and *E units*, seven-membered rings at the boundaries which act as an interface between the {311} defect and perfect crystal.[7] Usually ion implantation and annealing lead to the formation of long but narrow {311} defects (of just a few interstitial chains), known as *rodlike defects* (RLDs), while high-dose electron irradiation produces much wider structures.[2,6] Apart from the experimental characterization of these extended defects, many theoretical investigations on their structure, energetics, and induced strain fields have been published.[7–11]

Although {311} defect structure and energetics are well known, still there is not a clear picture about its formation mechanism from point defects mainly because small agglomerates (under 40 interstitials) cannot be resolved by TEM.[2] It has been postulated[12] that following implantation and/or during the ramping up of the anneal, most interstitial defects are in the form of di-interstitials, which are fast diffusing species.[13] It is suspected that precursors of {311} defects might exist, more complex than simply di-interstitials, although their exact nature is not known.[14] From photoluminescence and TEM studies it has been deduced that the transition from these precursors into {311} defects requires both a threshold fluence (1×10^{13} cm^{-2}) and temperature (600 °C) and that it involves a severe structural transformation.[15] Various authors have proposed, using theoretical calculations, particular interstitial clusters as seeds for the generation of {311} defects.[16–18] In a recent work, Du *et al.*[19] showed that compact tri-interstitial clusters can transform into ⟨110⟩ chain tetrainterstitials when capturing free self-interstitial defects. Those can further grow by capturing new free interstitials, but only in conditions of high interstitial supersaturation, since the chain tetrainterstitial rapidly relaxes into the compact tetrainterstitial[16] which is very stable and does not grow along ⟨110⟩. Other authors describe creation of {311} defects as the result of the coordinated generation of long interstitial chains and switching of atomic bonds,[7,11] a picture rather unrealistic.

In this Brief Report we demonstrate, using classical molecular dynamics (MD) simulation techniques, that precursors formed by chains of Si di-interstitials are metastable and spontaneously transform into {311} defects when annealed at high temperatures. Although we have carried out our simulations in Si specifically, our results are also applicable to Ge, where electron and ion irradiation also produce the generation of extended {311} defects.[6]

In our MD simulations we have used the Tersoff 3 potential,[20] which has been shown to give a good description of both point defects and Si structures different from perfect diamond.[21,22] In particular, structural and energetic properties of interstitial defects ranging from the single self-interstitial up to the very stable tetrainterstitial as described by Tersoff 3

 ©2008 The American Physical Society

are in very good agreement with results obtained using more fundamental techniques.[21–24] A limitation attributed to the Tersoff 3 potential is that it predicts a melting point temperature for Si of around 2400 K,[25] well above the value found in the experiments, 1685 K.[26] This is not an important drawback since it is possible to make a rescaling between real and Tersoff 3 temperatures. Porter *et al.*[27] related the simulation temperature T_{T3} with a scaled real temperature T_{real} by requiring that the internal energy of the classical simulation system at T_{T3} be equal to that of a corresponding quantum system at T_{real}. They defined a temperature-scaling expression based on a fifth-order polynomial that related T_{T3} with T_{real} up to $T_{\mathrm{real}}=700$ K. In a previous work where we studied the configurational and energetic properties of the Si self-interstitial we expanded their scaling law with a second-order polynomial.[23] We fitted the polynomial parameters by assuring continuity of the scaling law and its first derivative at $T_{\mathrm{real}}=700$ K and making the real melting temperature of 1685 K coincident with the Tersoff 3 melting temperature of 2400 K. With this scaling law, our results regarding self-interstitial diffusion were in very good agreement with experiments, showing that the dynamics of the system is adequately described in the full temperature range. In the following we will be referring to real temperatures.

Due to the particular orientation of {311} defects, in our MD cell we have chosen the X, Y, and Z axes to lie along the $[2\bar{3}\bar{3}]$, [311], and $[0\bar{1}1]$ directions, respectively. The smallest orthorhombic unit cell[9] that can reproduce the diamond Si lattice with this particular axis orientations contains 44 atoms and is of size $a\sqrt{11}/\sqrt{2}\times a\sqrt{11}\times a/\sqrt{2}$, being a the lattice constant of diamond Si (5.43 Å). We have used different MD cell sizes to accommodate each possible defect. In the particular case of RLD simulations we used $5\times3\times8$ unit cells, and for the wider {311} defect simulations we used $8\times3\times6$ unit cells. We applied periodic boundary conditions along the X and Z axes and free boundary conditions along the Y axis for allowing the volume relaxation of the MD cell (only expansion along the [311] direction is expected due to the particular displacement vector of the {311} defect). We have carried out annealing simulations at temperatures between 1200 and 1400 K, high enough to accelerate system dynamics but much lower than the melting point of diamond Si. During the structural transformation energy is freed in the form of latent heat. If no special care is taken to eliminate such excess heat (that in real silicon would dissipate trough the lattice), it remains within the MD cell due to periodic boundary conditions. To avoid such an artificial temperature increase, atom velocities were rescaled every 1000 time steps to maintain a constant temperature in the cell. We have used the fourth-order Gear predictor-corrector algorithm[28] to integrate equations of motion.

The tetrahedral interstitial is the lowest formation energy configuration within the Tersoff 3 description of silicon, with 3.45 eV.[23] In a previous work we showed that when two tetrahedral interstitials interact to form a di-interstitial, a bond defect (BD) is generated between them and the formation energy is lowered to 3.16 eV per interstitial atom.[25] The BD consists of a local rearrangement of bonds in the silicon lattice without any excess or deficit of atoms.[22] The atomic

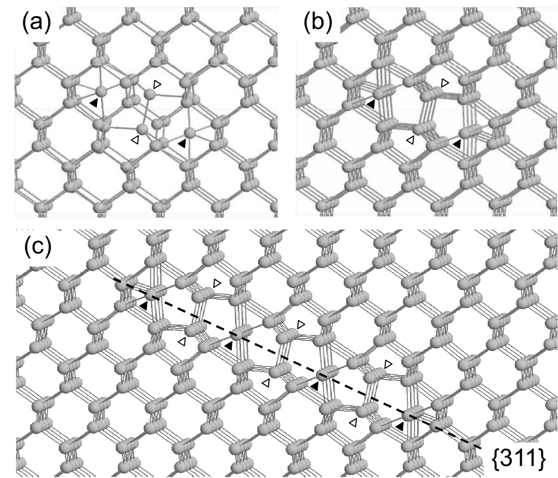

FIG. 1. Ball and stick models of (a) the Si di-interstitial, (b) a linear defect with one BD chain and eight Si interstitials, and (c) a planar defect with three BD chains and 16 Si interstitials. Solid and open triangles indicate Si interstitials and BD atoms, respectively.

structure of the Si di-interstitial is shown in Fig. 1(a). By repeating the Si di-interstitial structure (interstitial-BD-interstitial), extended defects can be generated. In Fig. 1(b) we show a defect generated by repeating the di-interstitial structure along the ⟨110⟩ direction. It can be described as two rows of interstitial atoms and one row of BDs in between. Analogously, additional BDs and Si interstitials can be added at both sides. This procedure generates planar defects as the one shown in Fig. 1(c). Interestingly enough, its habit plane is precisely the {311} plane.

We have analyzed different Si interstitial and BD arrangements (in length along ⟨110⟩ and width along ⟨311⟩). In Fig. 2 we show their calculated formation energy as a function of defect size for structures with 2, 3, 4, and 5 Si interstitial chains with BDs in between. In all cases, formation energies are lower than the corresponding to the tetrahedral self-interstitial and are a decreasing function of defect size. This indicates that it is energetically favorable to form these defects in comparison to having isolated self-interstitials in the

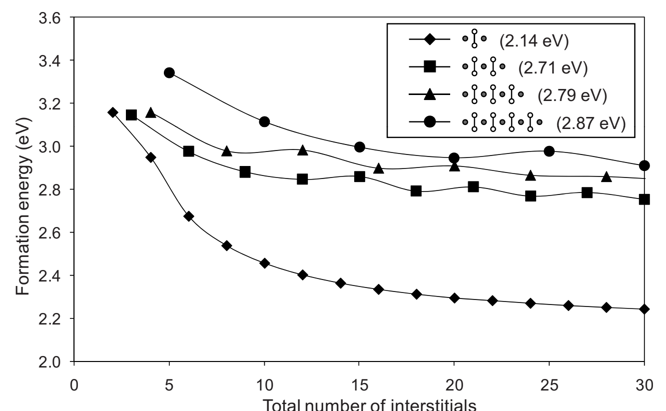

FIG. 2. Formation energy per interstitial atom as a function of size for defects formed by alternating ⟨110⟩ chains of interstitials (gray circles) and BDs (open circles). Energies in the legend correspond to infinite defects along ⟨110⟩.

lattice and also that once formed they will grow in size by capturing free self-interstitials. It is worth to note that in defects with more than one BD row the curves show small steps. These are due to pairing of interstitial atoms in the inner chains, which lowers the formation energy when the number of interstitials is even with respect to when it is odd.

From all curves shown in Fig. 2, the one with just one BD row shows the lowest formation energies. This indicates that interstitials will first arrange along the ⟨110⟩ direction giving rise to linear defects, as it is observed in the experiments of ion irradiation.[2] Using parallel replica dynamics, Birner *et al.*[29] observed that as Si interstitials are captured by RLD defects they diffuse to the chain ends producing its growth in length. If the Si interstitial supersaturation is very high, as it occurs in the case of high-dose electron irradiation experiments,[6] the RLD is likely to capture two or more Si interstitials. When these meet before reaching the edges, they become bonded together (the pairing of interstitials that produce the steps in Fig. 2) and make the defect to grow in width. This also happens if the RLD captures di-interstitials. This would explain why wide planar ⟨311⟩ defects are observed after heavy electron irradiation.

These defects formed by chains of Si interstitials and BDs are metastable at room temperature but undergo a structural transformation when annealed at higher temperatures. In Fig. 3 we show several snapshots taken during the heating at 1200 K of a linear interstitial defect with just one BD row, as the one shown in Fig. 1(b). This defect behaves as of being of infinite length along the ⟨110⟩ direction since, as we mentioned above, periodic boundary conditions are applied in *Z*. After 2.6 ns of annealing, the defect has transformed into a periodic structure along ⟨110⟩ that shows one rod of hexagonal Si in the center, surrounded by three seven-membered rings and three five-membered rings. All atoms are fourfold coordinated, and bond lengths and bond angles are not much distorted with respect to the perfect diamond lattice. In this configuration the formation energy of the defect has lowered to 1.50 eV per interstitial atom, in very good agreement with previous theoretical calculations using tight-binding techniques.[9,10] This structure is regarded as the basic RLD, formed by just two interstitial chains.[9–11] Figure 3(d) shows how atoms rearrange during the structural transformation. It is important to note that this is just the simplest possible rearrangement; in practice atoms may exchange positions even when they belong to different atomic layers along *Z*.

Figure 4 shows several snapshots taken during the annealing at 1400 K of a planar defect formed by 11 BD rows and 12 interstitial rows, being also infinite in *Z*. After 4 ns, it has spontaneously transformed into a {311} defect. Its structure, from left to right, is *EIIOIOIIIE*, and its formation energy of only 0.98 eV per interstitial atom, in good agreement with experiments[1,3] and theoretical calculations.[8–11] In Figs. 4(d)–4(f) we show how atoms rearrange. Again, this is only a simplified scheme since in practice atoms significantly move along the *Y* direction (as we shall see below) and some of them in *Z* direction as well. It is worth to note that the positions of BDs are not altered, although their constituent atoms can be exchanged during the transformation by atoms that previously occupied interstitial positions. This scheme would predict a 50% ratio between *I* and *O* units, but in fact the defect width shrinks during the transformation to a final 75% ratio between *I* and *O* units. This is in fair agreement with experiments, where a ratio of 62% has been found[6] (the difference of 13% is due to our defect being much narrower than the {311} defects observed by Takeda;[6] in fact, very narrow defects show no *O* units at all[31]). Theoretical calculations have shown that the separation of *O* units between one, two, or three *I* units observed in TEM acts so as to relax the strain energy introduced in the Si lattice by the *I* units.[7,10]

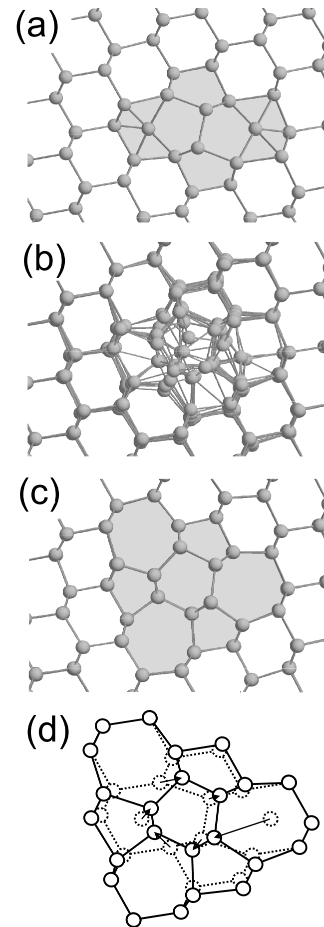

FIG. 3. *XY* snapshots taken during annealing at 1200 K of a linear defect: (a) initial configuration, (b) at 1.6 ns, and (c) final configuration at 2.6 ns (see Ref. 30). Defect areas in the initial and final configurations are shadowed for clarity. Scheme in (d) indicates how atoms rearrange during the transformation.

In some of our {311} generation simulations we observed the formation of an atomic rearrangement different from the ones reported by Takeda,[6] which is shown in Fig. 5. It contains two interstitial chains since it transforms into the *OI* unit arrangement by switching the bonds indicated in the schematics. Consequently, we will refer to this found structure as *OI′* arrangement. The atomic structure of its core resembles the one of the tetrainterstitial.[16,32,33] It is difficult to calculate the formation energy associated with *OI′* since, as it is known from previous theoretical calculations,[7,9] it will depend on the surrounding structural units. We have made an estimation by comparing with a sample consisting of one *OI* arrangement surrounded by the same structural units as the *OI′* shown in Fig. 5 (*I* units on both sides). We

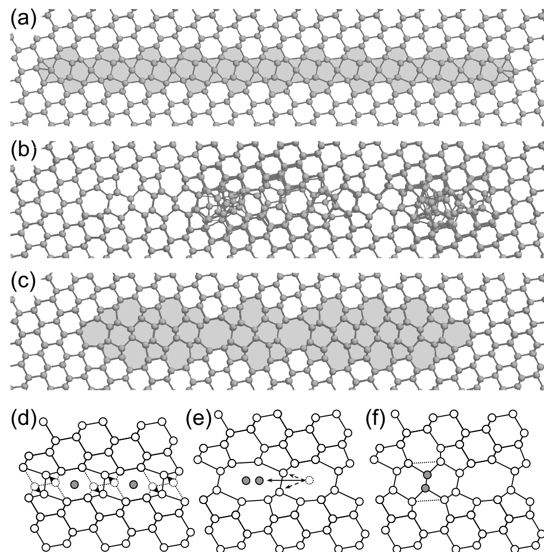

FIG. 4. *XY* snapshots taken during annealing at 1400 K of a planar defect: (a) initial configuration, (b) at 2.5 ns, and (c) final configuration at 4 ns (see Ref. 30). Defect areas in the initial and final configurations are shadowed for clarity. Below, scheme showing the stages in the transformation: (d) initial configuration with BD and interstitial (gray) chains, (e) lattice expansion and atom rearrangement, and (f) final configuration with a *I* unit on the left and a *O* unit on the right.

found no significant difference in the associated energies. However, higher strain is expected for OI' since it introduces in the lattice more bond length and angle distortions than the *OI* arrangement,[7,16] which would favor in practice the formation of the latter instead of the former.

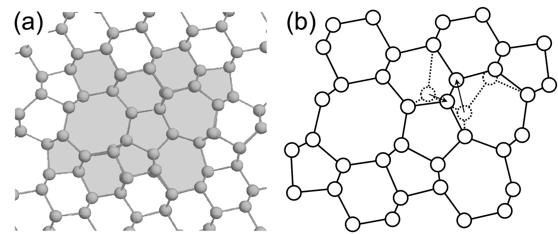

FIG. 5. (a) ⟨110⟩ projection of the atomic structure of the OI' arrangement (shaded; see Ref. 30). (b) Transformation from an *OI* arrangement (dotted) to a OI' arrangement (solid).

In conclusion, using MD techniques we have demonstrated the spontaneous transformation of interstitial-rich precursors into {311} defects when annealed at high temperatures. Their structure is based on the Si di-interstitial defect, consisting of ⟨110⟩ chains of interstitials and bond defects alternated along the {311} plane. This picture is in agreement with experimental observations which suggested that {311} generation is the consequence of a severe structural transformation from interstitial-rich precursors. Structure and energetics obtained from our simulations are in good agreement with previous first-principles and tight-binding calculations. However, it is worth to note that in such calculations the {311} structure was used as an input, while in our simulations it is the outcome. A {311} atomic structure, containing two ⟨110⟩ interstitial chains but arranged differently in comparison with a sequence of *O* and *I* units, has been found and analyzed.

This work has been supported by the Spanish DGI under Project No. TEC2005-05101.

*lmarques@ele.uva.es

[1] N. E. B. Cowern *et al.*, Phys. Rev. Lett. **82**, 4460 (1999).
[2] A. Claverie *et al.*, Appl. Phys. A: Mater. Sci. Process. **76**, 1025 (2003).
[3] D. J. Eaglesham *et al.*, Appl. Phys. Lett. **65**, 2305 (1994).
[4] J. P. Goss *et al.*, Appl. Phys. Lett. **85**, 4633 (2004).
[5] W. L. Ng *et al.*, Nature (London) **410**, 192 (2001).
[6] S. Takeda, Jpn. J. Appl. Phys., Part 2 **30**, L639 (1991).
[7] M. Kohyama and S. Takeda, Phys. Rev. B **46**, 12305 (1992).
[8] M. Kohyama and S. Takeda, Phys. Rev. B **51**, 13111 (1995).
[9] J. Kim *et al.*, Phys. Rev. B **55**, 16186 (1997).
[10] P. Alippi and L. Colombo, Phys. Rev. B **62**, 1815 (2000).
[11] J. P. Goss *et al.*, J. Phys.: Condens. Matter **14**, 12843 (2002).
[12] J. W. Corbett *et al.*, Nucl. Instrum. Methods **182-183**, 457 (1981).
[13] S. K. Estreicher *et al.*, Phys. Rev. Lett. **86**, 1247 (2001).
[14] H. G. A. Huizing *et al.*, Appl. Phys. Lett. **69**, 1211 (1996).
[15] S. Coffa *et al.*, Appl. Phys. Lett. **76**, 321 (2000).
[16] N. Arai *et al.*, Phys. Rev. Lett. **78**, 4265 (1997).
[17] M. M. De Souza *et al.*, Phys. Rev. Lett. **83**, 1799 (1999).
[18] D. A. Richie *et al.*, Phys. Rev. Lett. **92**, 045501 (2004).
[19] Y. A. Du *et al.*, Eur. Phys. J. B **57**, 229 (2007).
[20] J. Tersoff, Phys. Rev. B **39**, 5566 (1989).
[21] S. Munetoh *et al.*, Phys. Rev. Lett. **86**, 4879 (2001).
[22] L. A. Marqués *et al.*, Phys. Rev. Lett. **91**, 135504 (2003).
[23] L. A. Marqués *et al.*, Phys. Rev. B **71**, 085204 (2005).
[24] L. A. Marqués *et al.*, Phys. Rev. B **76**, 153201 (2007).
[25] L. A. Marqués *et al.*, Phys. Rev. B **64**, 045214 (2001).
[26] J. W. Mayer and S. S. Lau, *Electronics Materials Science for Integrated Circuits in Si and GaAs* (MacMillan, New York, 1990).
[27] L. J. Porter *et al.*, J. Appl. Phys. **81**, 96 (1997).
[28] C. W. Gear, *Numerical Initial Value Problems in Ordinary Differential Equations* (Prentice-Hall, Englewood Cliffs, NJ, 1971).
[29] S. Birner *et al.*, Solid State Commun. **120**, 279 (2001).
[30] See EPAPS Document No. E-PRBMDO-78-156839 for configuration files in Rasmol *xyz* format (atom type, *x*, *y*, and *z* coordinates in angstrom and potential energy in eV). For more information on EPAPS, see http://www.aip.org/pubservs/epaps.html.
[31] S. Takeda and T. Kamino, Phys. Rev. B **51**, 2148 (1995).
[32] M. Kohyama and S. Takeda, Phys. Rev. B **60**, 8075 (1999).
[33] B. J. Coomer *et al.*, J. Phys.: Condens. Matter **13**, L1 (2001).